HAMADRYAD
Accepted Manuscript

Title Phylogenetic position and osteology of a population of *Mysticellus franki* Garg & Biju, 2019 (Anura: Microhylidae) from south of the Palghat Gap, Western Ghats, India

Authors K.P. Dinesh[1], Varun R. Torsekar[2], Jaimi A. Gray[3], Kartik Shanker[2], David C. Blackburn[4]

[1]Zoological Survey of India, Western Regional Centre, Pune, Maharashtra, India
[2]Centre for Ecological Sciences, Indian Institute of Science, Bangalore, Karnataka, India
[3]The University of Texas at Austin, Department of Earth and Planetary Sciences, 2275 Speedway Stop C9000, Austin, TX 78712-1722, USA
[4]Florida Museum of Natural History, University of Florida, 1659 Museum Road, Gainesville, Florida 32611 USA

* Corresponding author email: kpdinesh.zsi2@gmail.com

Date submitted 18/09/2024

Date accepted 21/08/2025

Available online

Citation Dinesh, K.P., Torsekar, V.R., Gray, J.A., Shanker, K. and Blackburn, D.C. (2025) Phylogenetic position and osteology of a population of *Mysticellus franki* Garg & Biju, 2019 (Anura: Microhylidae) from south of the Palghat Gap, Western Ghats, India. *Hamadryad* in press

Abstract *Mysticellus franki* is a rare and a little-studied microhylid frog which was described in 2019 from the central Western Ghats. The species was originally described from the Wayanad hill ranges, north of the Palghat Gap. Here, we report a shallow divergent lineage from south of the Palghat Gap. Using a single specimen collected during 2012, we present osteological data along with phylogenetic and morphological data to provide a more comprehensive understanding of this rare species.

Keywords Computed tomography, Endangered species, Shallow divergence

Introduction

The globally distributed anuran family Microhylidae is represented in India by nearly 30 species in seven genera (Dinesh, et al. 2024; Ramakrishna et al. 2023), including the recent addition of the monotypic genus *Mysticellus* Garg and Biju, 2019 (Dinesh, 2020; Ramakrishna et al. 2023). Cyriac et al. (2024) noted the difficulties in reconstructing the history of diversification for lineages such as *Mysticellus* that are represented by a single species.

Mysticellus franki was described by Garg and Biju (2019) based on six adult specimens collected on 5 June 2015 from the Suganthagiri region of Wayand plateau, Kerala, Western Ghats (Garg and Biju, 2019). At the time, this species was known only from the type locality and a single collection event. The species may have gone unnoticed by the scientific community for a long time due its superficial morphological resemblance to the common microhylid frog *Microhyla rubra*. Garg and Biju (2019) reported species congregations for breeding around temporary muddy pools during the initial monsoon showers. Subsequently, a photographic record of *M. franki* from Nelliyampathy Hills (Kesavapara) was obtained in October 2023 by Agashe et al. (2023) during their field studies. However, they did not collect a specimen to facilitate comparisons with the collections of Garg and Biju (2019) from the Suganthagiri region of Wayanad.

In the phylogenetic analysis by Garg and Biju (2019), *M. franki* was recovered as sister to members of the genus *Micryletta*, which is distributed in the Andaman and Nicobar Islands, northeastern India, Taiwan, China, Malaysia, and Indonesian Sumatra (Frost, 2024). Garg and Biju (2019) found that the divergence of *M. franki* from *Micryletta* occurred during the Eocene, suggesting that this lineage represents a more recent arrival into India than other relict lineages of the Western Ghats, including the families Micrixalidae, Nasikiabatrachidae, Nyctibatrachidae, and Ranixalidae. Other than the photographic record from Kesavapara , Nelliampathy (Agashe et al 2023), no other information is available for this population south of the Palghat Gap.

In 2012, we (VT, KPD) collected a single adult male individual (with an externally visible vocal sac) of *Mysticellus* during our large-scale amphibian studies in the Western Ghats. Here, we provide a confirmed (specimen based) record of a new population of *M. franki* from south of the Palghat Gap. We examine the genetic divergence of *M. franki* from south of the Palghat Gap with the type locality and provide the first description of osteology for the genus *Mysticellus*. Additionally, because *Micryletta* is the sister clade to *Mysticellus* (Fig 6), we compare the osteology of *M. franki* (CESF2751) with *Micryletta inornata* (based on CAS:Herp:2315241).

Material and Methods

As a part of our amphibian explorations in the Western Ghats, field sampling was carried out around the Nelliampathy hill ranges and Anamalai massifs that are south of Palghat Gap. One individual (CESF2751, deposited in the CES, IISc, Bangalore) was collected late in the evening on 1 July 2012, near Meenampara, Nelliyampathy (N 10.53877, E 76.7075) and was photographed *in situ* to record its colouration, following which the specimen was euthanized using MS222, fixed in 4% formalin, and preserved in 70% alcohol. For genetic analysis, liver tissue sample was stored in molecular grade alcohol. Natural history and habitat data were collected from the field.

Morphological measurements and abbreviations are as follows: AG — axilla to groin distance; BW — body width; ED — eye diameter, i.e. the horizontal distance between the bony orbital borders of the eye; EN — eye to nostril distance; ES — eye to snout tip distance; f1, f2 — finger I and II length (tip of finger to proximal palmar tubercle); FEL — thigh length, measured from the cloaca to the obtuse margin of the knee; FOL — foot length, measured from the base of the inner metatarsal tubercle to the tip of the fourth toe; HL — head length, from the rear of the mandible to the tip of the snout; HW — head width, at the angle of the jaws; IBE — distance between posterior corner of eyes; IFE — distance

between anterior corner of eyes; IN — internarial distance; IO — inter-orbital distance, measured as the distance between the mid-point of the upper eyelids; LAL — lower arm length , measured from the elbow till the posterior edge of the outer metacarpal tubercle ; MAE — distance between the mandibular angle to the anterior eye margin; MPE — distance between the mandibular angle to the posterior eye margin; PAL — palm length, measured from the posterior edge of the outer metacarpal tubercle to the tip of the third finger; SVL — snout to vent length; t4 — toe 5 length, measured from base of proximal sub articular tubercle to toe tip; TAR — tarsus length, measured from the obtuse margin of the tibio-tarsal articulation to the posterior end of the inner metatarsal tubercle; TBL — shank length, measured from the obtuse margin of the knee to the obtuse margin of the tibio-tarsal articulation; UAL — upper arm length, measured from the axilla to the obtuse margin of the elbow; UEW — maximum width of the upper eyelid were measured using Mitutoyo vernier callipers (to the nearest 0.1 mm) and the LEICA MZ75 microscope (0.63 magnification under 1X objective). Institutional abbreviations are as follows: CAS:Herp — California Academy of Sciences, Department of Herpetology, California, USA; CES — Centre for Ecological Sciences; IISc—Indian Institute of Sciences, Bangalore, India.

We extracted genomic DNA from the tissue (CESF2751) sample following the phenol-chloroform-isoamyl alcohol method of Sambrook et al. (1989). After purification of genomic DNA, mitochondrial 16S rRNA was PCR-amplified using 16Sar-L and 16Sbr-H primers (Simon et al. 1994), and a QIAquick® PCR Purification Kit was used to clean the PCR amplified product, which was then sequenced using a 3130xl Genetic Analyzer.

Forward and reverse sequences were verified manually in Chromas and aligned in MEGA X. For the phylogenetic reconstruction, sequences generated by Garg and Biju (2019) were downloaded from GenBank and analyzed with the sequences generated for the current study. Maximum Likelihood phylogenetic reconstruction (Fig. 2) was performed in IQ tree webserver (Trifinopoulos et al. 2016) with 1000 ultrafast bootstraps and SH-aLRT branch test under TIM2+F+I+G4 model auto selected according to Bayesian Information Criterion (BIC). The ML phylogeny was visualized by Fig Tree v1.4.0, treating members of *Glyphoglossus* as the outgroup.

Osteology

We used X-ray Computed Tomography (CT-scanning) to visualize the skeleton of this new specimen (CESF2751) of *Mysticellus*, as well as a representative of the closely related genus *Micryletta*. Scans of CESF2751 were produced at the GE India Industrial Pvt. Ltd. facility in Pune, India using a Phoenix v|tome|x M (GE's Measurement & Control business, Boston, MA, USA), with a 180 kV x-ray tube with a diamond-tungsten target and with the following settings: 60–80 kV, 300 mA, a one second detector time, averaging of three images per rotation, and a voxel resolution of 3.0–4.9 mm. We generated the CT-scan of *Micryletta inornata* (CAS:Herp:2315241) at the University of Florida Nanoscale Research Facility, also using a Phoenix v|tome|x M, as part of the openVertebrate Thematic Collections Network (Blackburn et al., 2014). All image stacks, associated metadata, and 3D mesh files are available on-line via MorphoSource (CESF2751 TIFF stack: https://doi.org/10.17602/M2/M19727, 3D mesh: https://doi.org/10.17602/M2/M19834; CAS:Herp:2315241 TIFF stack: https://doi.org/10.17602/M2/M46293, 3D mesh: https://doi.org/10.17602/M2/M163187). Our osteological terminology follows that of Trueb, Diaz & Blackburn (2011), though we refer to the manual digits as I–IV rather than II–V to avoid confusion for most taxonomists.

Results and Discussion

Detailed external morphological, genetic, and natural history data were previously provided for *M. franki* from the type locality by Garg and Biju (2019). Here, we provide additional details of external morphology, genetic distance, phylogenetic relationships, and osteology to evaluate this population of *Mysticellus* from south of the Palghat Gap.

Morphology

The morphology of the specimen collected (CESF2751) south of Palghat Gap largely matches the description of *M. franki* by Garg and Biju (2019) (Fig. 1): medium-sized microhylid frog (SVL = 23.5 mm) with squat body; head length less than head width (HL = 5.9 mm; HW = 7.8); snout acutely pointed (ES = 3.1 mm) and equal to eye diameter (ED = 2.9 mm); canthus rostralis angular, loreal region flat, inter orbital space flat (IO = 3.6 mm) and greater than upper eyelid width (UEW = 2.0 mm) and internarial distance (IN = 2.0 mm); distance between back of eyes greater than distance between front of eyes (IFE = 3.8 mm; IBE = 6.7 mm); nostrils oval, nearer to tip of snout; symphysial knob weak; tympanum invisible; supratympanic fold weak; post narial ridges moderately developed; tongue not emarginated without papilla. Lower arm slender and shorter (LAL = 6.1 mm) than palm (PAL = 7.2 mm); fingers short and thin without dermal fringes, relative finger length f1<f2<f4<f3 (f1 = 2.7 mm and f2 = 2.8), tips rounded, webbing between fingers absent; subarticular tubercles, pre-pollex tubercle and supernumerary tubercles distinct. Hind limbs short, thigh length sub equal to shank length (FEL = 10.9 mm; TBL = 10.4 mm); foot length greater than tarsus length (FOL = 12.0 mm, TAR = 5.6 mm), relative toe length I<II<III<V<IV (t4 = 6.8 mm); toe tips rounded; webbing primitive, inner metatarsal tubercle distinct and inner metatarsal tubercle moderate. Entire dorsum bronze brown, paler anterior and darker towards posterior (Fig. 2). Tip of snout below eye, shoulder, and lateral region blackish lateral banded pattern continuing to groin. Two blackish spots on dorsum in inguinal region, only visible when thigh abducted. Complete ventral region black speckled with white (Fig. 2). The dorsal colouration pattern matches the photographic record by Agashe et al. (2023).

Phylogenetics

As observed in Garg and Biju, (2019), CESF2751 is recovered as a sister lineage to *Micryletta* (Fig. 3) and exhibits shallow genetic divergence with the type locality population. The *Mysticellus* specimen from Nelliampathy Hills is 1.3% divergent from the population in the Wayanad hill ranges for the mitochondrial 16S rRNA gene (Garg and Biju, 2019). The two sequences (MK285340.1 and MK285346.1) generated by Garg and Biju (2019) from the Wayanad range are identical.

Osteology

Because the osteology of *M. franki* has not been described previously, we provide a basic description of the skeleton and general comparisons to one of the members (*Micryletta inornata*) of its sister genus *Micryletta*.

Based on CESF2751 (adult male; 23.5 mm SVL): The skull is lightly constructed, longer than it is wide, lacking ornamented dermal bones, and having jaw joints located in line with the anterior margin of the otic capsules. The prootics are ossified and synostosed to the exoccipitals and frontoparietals. The lateral walls of the neurocranium are ossified such that the optic fenestrae and prootic foramina are bounded by bone. The frontoparietals are broad, nearly as wide as they are long, and are separated throughout their lengths except at the posterior margins where they are weakly fused. The broad nasals meet at the midline, and may be partially synostosed to the underlying sphenethmoid. There are no teeth on the premaxillae, maxillae, or vomers. Each premaxilla has a slender alary process that is widely separated from the nasal. The maxillae are long, slender, and nearly straight. The quadratojugals articulate with the posterior portion of the maxilla, and extend anterior from the body of the squamosal. The pterygoids are slender and triradiate, with a slender anterior ramus that articulates with the maxilla, and a posterior ramus that extends just posterior of the jaw joint. The vomer is small, C-shaped, and synostosed to the ossified sphenethmoid, which has a well-ossified septum nasi. The parasphenoid is broad and triadiate, with a cultriform process that appears to be synostosed to the sphenethmoid. The squamosals are slender and with a minute zygomatic ramus, a small posterior ramus, and do not articulate with the prootic. A thin, bowed stapes (or columella) projects ventrally and anteriorly from the prootic; an ossified operculum is not present. The posteromedial process of the hyoid are robust, and expanded into a plate near the articulation with the hyoid plate.

The atlas and Presacral II are fused, and Presacrals III–VIII are distinct, procoelous, and non-imbricating. The transverse processes of Presacral II are oriented anteriorly, those of Presacral III–V oriented posteriorly, those of Presacral VI laterally, and those of Presacrals VII and VIII anteriorly. Presacral VIII has a biconvex centrum, making the vertebral column displasiocoelous. The sacrum is procoelous with broad, triangular transverse processes, and two condyles posteriorly. The urostyle bears two cotyles that are confluent, and a short dorsal ridge that extends along the anterior third of the urostyle.

The pectoral girdle is firmisternal and lacks clavicles. The scapular has a weakly defined waist and expands dorsally. The coracoid is expanded medially, with the medial extent approximately twice as wide as the lateral extend. There is no omosternum, as well as no mineralized or ossified sternal elements.

The three elements of the pelvic girdle — ilium, ischium, and pubis — are ossified and synostosed. The shaft of the ilium is long and mostly straight, with a well-defined but small dorsal protuberance, and without a supraacetabular fossa or dorsal crest. The synostosis of the pelvic elements creates a broad, semi-circular bony plate that is approximately constant in its width posterior, ventral, and anterior to the acetabulum.

The humerus is thin and weakly bowed with a short ventral crest and well-defined entepicondyle. The forearm is approximately 90% of the length of the humerus. The radiale and ulnare are approximately equal in size. Distal carpals 3+4+5 are fused, and Element Y and distal carpal 2 are distinct and unfused. The phalangeal formula for the manus is 2-2-3-3. The tibiofibular and femur are similar in length. There are two distal tarsals and a single small, conical prehallux. The phalangeal formula for the pes is 2-2-3-4-3. There may be small subarticular sesamoids at the metacarpophalangeal, metatarsophalangeal, and interphalangeal joints, but the resolution of the CT-scan was not sufficient for determining this. The terminal phalanges taper distally, giving a thin, triangular appearance, often with as small knob distally. The skeletons of *M. franki* (CESF2751) and *Micryletta inornata* (CAS:Herp:231524, from Myanmar) are generally similar. Both lack teeth, lack a clavicle, and have similar proportions of the head, limbs, and body. The atlas and Presacral II are fused in *Mysticellus*, but not in *M. inornata.* There is also a distinct vomer in *M. inornata* that is widely separated from the ossified sphenethmoid; the vomer is fused to the sphenethmoid in *Mysticellus*. The pectoral girdles are similar, but there is evidence for mineralized sternal cartilages in *M. inornata*. The phalangeal counts and shapes are similar between the two genera, but *M. inornata* has a bipartite prehallux. Both genera have long, slender stapes that are directed anteriorly, but the stapes of *Mysticellus* is directed ventrally whereas that of *M. inornata* is directed more laterally. The ventrally directed stapes of *Mysticellus* is unusual and its significance unclear.

Geography

The type locality of *M. franki* Garg and Biju (2019) is aerially 130 km from the collection locality of the specimen described here, and these individuals exhibit shallow genetic divergence across the Palghat Gap. Our collection locality is 5 km aerially away from the new locality reported by Agashe et al. (2023) which is from the adjacent hill ranges (Kesavapara) (Fig. 3).

This is only the third report of the species from the Western Ghats and second south of the Palghat Gap. The species was collected from Wayanad at 800 m and from Nelliampathy at 1100 m, and is thus expected to occur at these elevations in the hill ranges between these two locations. IUCN (2023) treated *M. franki* as "Critically Endangered" B1ab(iii) based on its extent of occurrence (EOO) of 2 km^2 since the species was known only from one location. With three confirmed records for *Mysticellus*, the EOO is approximately 225.11 km^2. This will likely increase with additional locations as the width of the polygon representing the EOO is currently very narrow. Based on these range estimates, the IUCN status of the species may now warrant an 'Endangered' status, which may also need to be revised based on additional records.

Our record of *M. franki* from the southern Western Ghats exhibits a shallow genetic divergence (1.3% on mitochondrial 16s rRNA) from the northern specimens. Population structuring among the two populations is likely due to the Palghat Gap serving as a phylogeographic barrier. Previous phylogenetic analysis (Garg and Biju, 2019) suggests a sister relationship between the genera *Mysticellus* (in the central and southern Western Ghats, India) and *Micryletta* (in Taiwan, China, West Malaysia, Sumatra, and India including Northeast India and Andaman and Nicobar Islands (Frost, 2024)). The first osteological observations for *M. franki* suggest a strong similarity in the skeletons of these two genera, although they also reveal a notable difference (the orientation of the columella), which suggests some difference in the auditory biology of the two genera.

Acknowledgements

The authors are grateful to the Kerala State Forest Department for fieldwork and collection permits. We acknowledge the support of Saunak Pal, S.R. Chandramouli, and Priyanka Swamy in the field and laboratory. We are grateful to S.P. Vijayakumar for his help and support in generating the osteological data. We are thankful to P. Deepak for the geocoordinate map. KPD is the grateful to the Director, Zoological Survey of India (ZSI), Kolkata and the Officer-in-Charge, ZSI, WRC, Pune for their support.

References

Agashe, M., Ghosh, A., Dilshad, K., Sil., M. & Datta-Roy, A. (2023) New distribution records of two uncommon microhylid frogs, *Melanobatrachus indicus* Beddome, 1878 and *Mysticellus franki* Garg & Biju, 2019 from Nelliyampathy, Kerala, India. *Journal of Threatened Taxa*, 15, 22900–22904. https://doi.org/10.11609/jott.8300.15.3.22900-22904

Bachman, S., Moat, J., Hill, A.W., De La Torre, J. & Scott, B. (2011) "Supporting Red List threat assessments with GeoCAT: geospatial conservation assessment tool." In: Smith V, Penev L (Eds), *e-Infrastructures for data publishing in biodiversity science. ZooKeys*, 150, 117–126. (Version BETA)

Cyriac, V.P., Ashwini, V.M., Dinesh, K.P., Torsekar, V., Jayarajan, A., Swamy, P., Vijayakumar, S.P., And Shanker, K. (2024) Diversifying in the mountains: spatio-temporal diversification of frogs in the Western Ghats biodiversity hotspot. *Evolution*, qpae006, https://doi.org/10.1093/evolut/qpae006 .

Dinesh. K.P. (2020) Amphibia. *In*: Chandra, K., Raghunathan, C., Sureshan, P.M., Subramanian, K.A. and Rizvi, A.N (Eds.), *Faunal Diversity of Biogeographic Zones of India: Western Ghats*: 1–744 (Published by the Director Zoological Survey of India, Kolkata) (ISBN 978-81-8171-566-1).

Dinesh.K.P., Deuti, K. And Saikia, B. (2024) *Checklist of Fauna of India: Animalia: Chordata: Amphibia*. Version 1.0. Zoological Survey India. DOI: https://doi.org/10.26515/Fauna/1/2023/Chordata:Amphibia

Frost, D. R. (2024) *Amphibian Species of the World: an Online Reference*. Version 6.2 (Date of access, 24/07/2024). Electronic Database accessible at https://amphibiansoftheworld.amnh.org/index.php. American Museum of Natural History, New York, USA. doi.org/10.5531/db.vz.0001

Garg, S. & Biju, S.D. (2019) New microhylid frog genus from Peninsular India with Southeast Asian affinity suggests multiple Cenozoic biotic exchanges between India and Eurasia. *Scientific Reports*. 9. 10.1038/s41598-018-38133-x.

IUCN. (2023) The IUCN Red List of Threatened Species. Version 2023–1. Available at: www.iucnredlist.org. (Accessed: 07 December 2023).

Ramakrishna, Deepak, P. And Dinesh, K.P. (2023) Status of Amphibian Diversity in the Western Ghats. In: T. Pullaiah (Eds) *Biodiversity Hotspot of the Western Ghats and Sri Lanka*. Published by CRC Press, Taylor and Francis Group: pp 219–240, (ISBN ebook: 9781003408758).

Sambrook, J., Fritsch, E.F. & Maniatis, T. (1989) *Molecular Cloning: A Laboratory Manual.* Cold Spring Harbor Laboratory Press, Nova York, 1626 pp.

Simon, C, Frati, F., Beckenbach, A., Crespi, B., Liu, H. & Flook, P. (1994) Evolution, weighting and phylogenetic utility of mitochondrial gene sequences and a compilation of conserved polymerase chain reaction primers. *Annals of the Entomological Society of America*, 87(6), 651–701. https://doi.org/10.1093/aesa/87.6.651

Trifinopoulos, J., Nguyen L.T., Haeseler, A.V. & Minh, B.Q. (2016) W-IQ-TREE: a fast online phylogenetic tool for maximum likelihood analysis, *Nucleic Acids Research*, 44 (1): 232–235. https://doi.org/10.1093/nar/gkw256

Ttueb, L., Diaz, R., & Blackburn, D. C. (2012) Osteology and chondrocranial morphology of *Gastrophryne carolinensis* (Anura: Microhylidae), with a review of the osteological diversity of New World microhylids. Phyllomedusa: *Journal of Herpetology*, 10(2), 99–135. https://doi.org/10.11606/issn.2316-9079.v10i2p99-135

Vijayakumar, S.P., Pyron, R.A., Dinesh, K.P., Torsekar, V., Srikanthan, A.V., Swamy, P., Stanley, E.L., Blackburn, D.C. & Shanker, K. (2019) A new ancient lineage of frog (Anura: Nyctibatrachidae: Astrobatrachinae subfam. nov.) endemic to the Western Ghats of Peninsular India. PeerJ 7: e6457 https://doi.org/10.7717/peerj.6457.

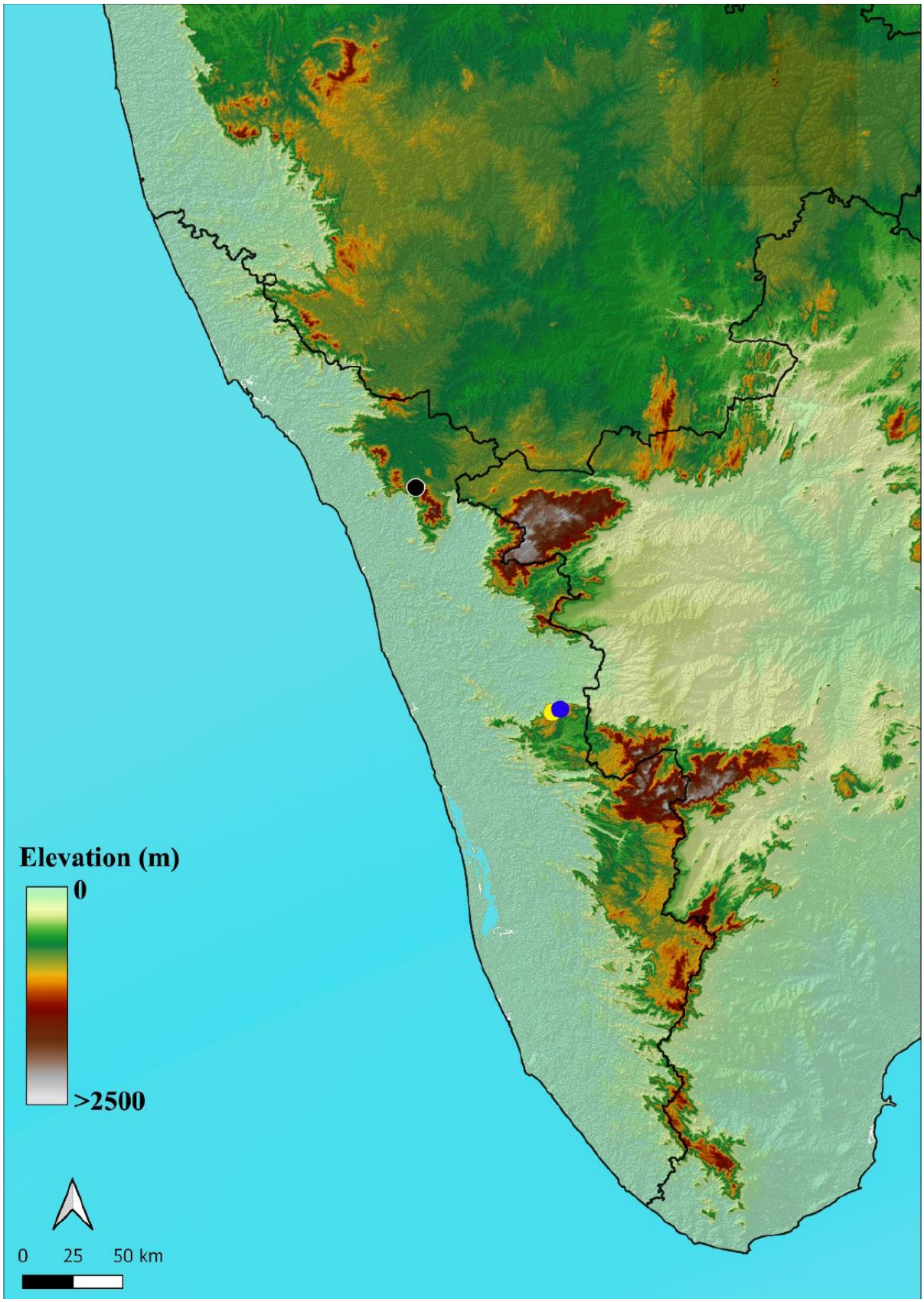

Figure 1: Map showing distribution record of *Mysticellus franki* in the central and southern Western Ghats, India (black circle type locality, blue circle photographic record from Kesavapara, and yellow circle shallow divergent population from Meenampara).

Figure 2: *Mysticellus franki* (CESF 2751) *in situ* from Neliyampathi hills, south of Palghat Gap, southern Western Ghats, India.

Figure 3: Dorsal and ventral images of *Mysticellus franki* (CESF 2751) *in situ* from Neliyampathi hills, south of Palghat Gap, southern Western Ghats, India.

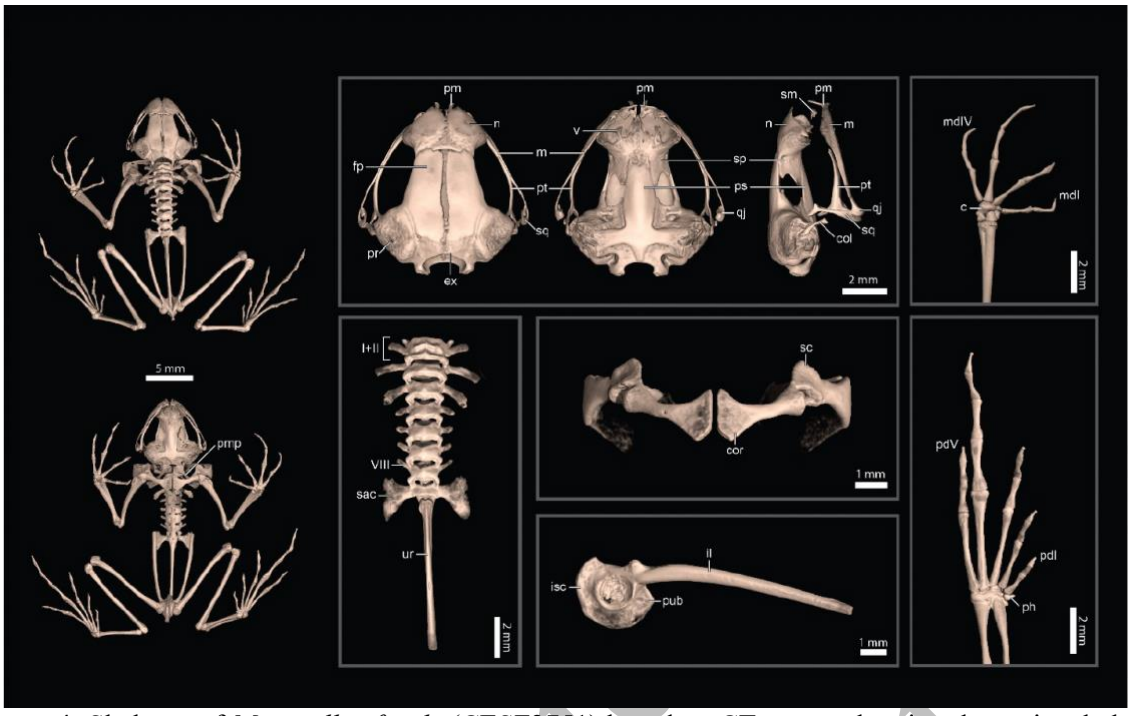

Figure 4: Skeleton of *Mysticellus franki* (CESF2751) based on CT-scans, showing the entire skeleton in dorsal and ventral views, the skull in dorsal, ventral, and lateral views, the vertebral column in dorsal view, the pectoral girdle in ventral view, the pelvic girdle in lateral view, the left manus in dorsal view, and the left pes in ventral view. Abbreviations: col, columella (stapes); c, carpals 3+4+5; cor, coracoid; ex, exoccipital; fp, frontoparietal; il, ilium; isc, ischium; m, maxilla; min, mineralized cartilage; n, nasal; ph, prehallux; pm, premaxilla; pmp, posteromedial process of the hyoid; pr, prootic; ps, parasphenoid; pt, pterygoid; pub, pubis; qj, quadratojugal; sac, sacrum; sc, scapula; ses, sesamoid; sp, sphenethmoid; sq, squamosal; v, vomer; ur, urostyle.

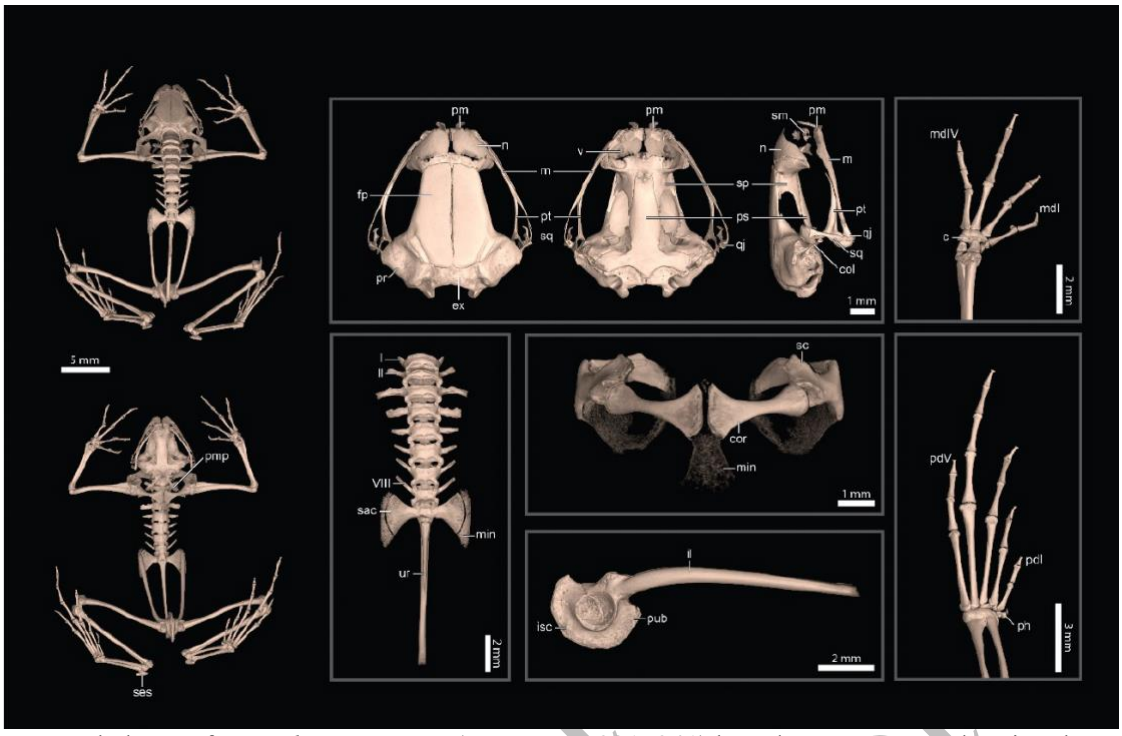

Figure 5: Skeleton of *Micryletta inornata* (CAS:Herp:2315241) based on CT-scans, showing the entire skeleton in dorsal and ventral views, the skull in dorsal, ventral, and lateral views, the vertebral column in dorsal view, the pectoral girdle in ventral view, the pelvic girdle in lateral view, the left manus in dorsal view, and the left pes in ventral view. Abbreviations as in Figure 4.

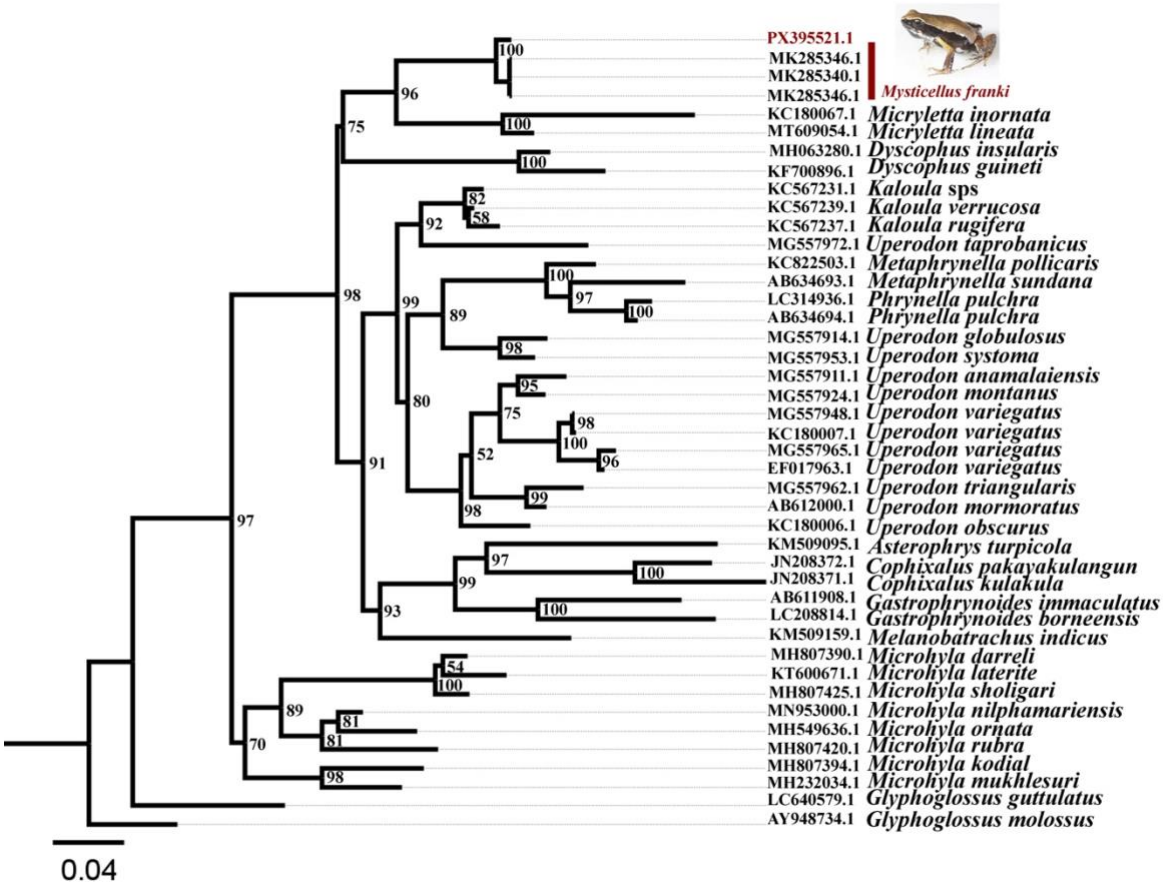

Figure 6: Maximum likelihood phylogeny for the species of *Mysticellus* based on 690 bp of 16S rRNA gene. Support values as nodes indicate values from non-parametric bootstrapping, and the scale bar is in units of substitutions per site.